^{1}H NMR Spectroscopy Characterization of Porcine Vitreous Humor in Physiological and Photoreceptor Degeneration Conditions

Alberto Elmi,[1] Domenico Ventrella,[1] Luca Laghi,[2] Giacomo Carnevali,[1] Chenglin Zhu,[2] Grazia Pertile,[3] Francesca Barone,[1,3] Fabio Benfenati,[4,5] and Maria Laura Bacci[1]

[1]Department of Veterinary Medical Sciences, University of Bologna, Bologna, Italy
[2]Centre of Foodomics, Department of Agro-Food Science and Technology, University of Bologna, Bologna, Italy
[3]Ophthalmology Department, Sacro Cuore Hospital - Don Calabria, Negrar, Italy
[4]Center for Synaptic Neuroscience and Technology, Italian Institute of Technology, Genoa, Italy
[5]Department of Experimental Medicine, University of Genoa, Genoa, Italy

Correspondence: Francesca Barone, Department of Veterinary Medical Sciences, University of Bologna, Via Tolara di Sopra, 50 Ozzano dell'Emilia, Bologna 40064, Italy; francesca.barone7@unibo.it.

AE and DV contributed equally to the work presented here and should therefore be regarded as equivalent authors.

PURPOSE. Qualitative and quantitative analysis of vitreous humor (VH) is important to discriminate between physiological and pathological conditions and may be particularly helpful when using animal models for ophthalmologic research. The aim of the present study was to investigate the physiological qualitative/quantitative composition of the VH of the standard pig using a metabolomics approach based on ^{1}H nuclear magnetic resonance (NMR) spectroscopy. A secondary aim was the characterization of the VH of the porcine model of photoreceptor degeneration induced with iodoacetic acid (IAA), widely used in the biomedical field, and comparison with the physiological one.

METHODS. VH samples were collected from 30 pigs (17 in the physiological condition and 13 treated with IAA) upon vitrectomy and analyzed by means of ^{1}H NMR spectroscopy for characterization.

RESULTS. On all analyzed samples, 40 molecules could be identified and quantified, with lactate being the most abundant in both physiological and photoreceptor degeneration conditions. Upon comparison, only 17 molecules showed statistical differences: In the IAA group, glucose and glutamine increased, while lactate, 4-amynobutyrate, hypoxanthine, dicarboxylic acids (succinate and fumarate), amino acids with their derivatives (creatine, alanine, valine, lysine, leucine, glycine, taurine, and isoleucine), and choline with its precursor sn-glycero-3-phosphocholine decreased.

CONCLUSIONS. The results validate the metabolic impairment determined by glycolysis inhibition upon systemic IAA administration. In conclusion, this work represents the first characterization of the porcine VH metabolome in physiological conditions and provides additional information for the characterization and refinement of the IAA-induced photoreceptor degeneration model.

Keywords: vitreous humor, photoreceptor degeneration, porcine model, 1H NMR spectroscopy, metabolomics

The vitreous humor (VH) is a highly hydrated (>98%) jellified extracellular matrix mainly constituted by different types of collagen fibrils,[1] in particular II, V/XI, IX,[2] and hyaluronan, a nonsulphate glycosaminoglycan (GAG) structure that fills the spaces between collagen fibrils.[3] The VH is considered to be virtually acellular except for the presence of a small number of hyalocytes.[4] When looking at its anatomic features, VH is enclosed in and attached to the pars plana of the retina and makes contact with the lens.[5] VH has different functions including mediating the metabolic requirements of the lens, stopping the leakage of cells and large macromolecules from the vascular stream into the vitreous cavity,[6] and acting as a diffusional barrier to the free movement of molecules between the anterior and posterior eye.[7] Furthermore, VH seems to act as a reservoir for several compounds unable to cross the blood–retinal barrier (BRB) such as proteins and other solutes.[8]

In recent decades, different studies have underlined the importance of the analysis of VH in order to find differences in its molecular composition during diverse physiological/pathological conditions[5] such as diabetes,[9] aging,[10] and retinal diseases[11] by means of different analytical approaches. Undeniably, qualitative and quantitative results are highly influenced by a correct sampling technique, which is actually obtained by vitrectomy during surgical procedures.[9] Metabolomics based on ^{1}H nuclear magnetic resonance (NMR) spectroscopy has proven to be one of the most favored and reliable approaches for in-depth qualitative and quantitative characterization of a variety of biological fluids in different species, including porcine species.[12–14] For example, a ^{1}H NMR-based topographical analysis of goat VH showed the existence of different

functional areas characterized by different metabolomic compositions, with main components represented by free amino acids, organic acids, osmolytes (such as myo-inositol and betaine), glucose, lactate, and ascorbate.[15] The study of the VH metabolome is important, beyond ophthalmology, also for internal medicine[5] and for forensic sciences.[16] In order to acquire more specific and robust data, animal models are extremely important and used widely in different fields of medicine.[7] Several species have been used for VH studies, including frogs,[17] cattle,[18] sheep,[19] and rabbits.[20] When approaching ophthalmologic research fields, it is easy to notice a marked increase in the use of the porcine model mainly due to its anatomic and functional similarities with the human.[21]

The importance of animal models of retinal degeneration and their value in the biomedical field has been widely recognized in recent years and has led to the development of different models.[22] To date, several porcine models of photoreceptor degeneration have been proposed,[23,24] including the transgenic miniature swine, for example, the TgP23H model of retinitis pigmentosa,[24] or induced by an intravenous injection of iodoacetic acid (IAA).[21,25,26] The latter chemical compound causes an inhibition of anaerobic glycolysis through the reaction with the glyceraldehyde-3-phosphate dehydrogenase.[27] Photoreceptors are affected by IAA injection in a dose-dependent manner (assessed between 7.5 and 12 mg/kg), with a decrease in production of energy and eventually death.[21] It has been proven that rods are distinctly more susceptible to such treatment when compared to cones, with their loss occurring in 3 to 5 weeks.[21,28] Extensive characterization and deep knowledge of such models are necessary in choosing which one to enroll in different experimental protocols, as any model has its own potential and usefulness. For retinal degeneration, for example, transgenic models may be more suitable when the goal is to study etiology and progression of the disease or approaches like gene therapy. On the other hand, chemically induced models, relatively cheaper and easier to obtain, may provide good results for the evaluation of surgical therapeutic approaches in the context of prostheses or regenerative medicine.[29]

In light of the need for model characterization and knowledge, the aim of the present study was to investigate the physiological qualitative/quantitative composition of the vitreous humor of the standard pig (VH$_p$) using a metabolomics approach based on ^{1}H NMR spectroscopy. A secondary aim was the characterization of the VH of the porcine model of photoreceptor degeneration induced with IAA (VH$_{pIAA}$) for its refinement and for comparison with the physiological condition.

Methods

Animals and Protocols

The use of the animals in this study was regulated by two protocols approved by the Italian Ministry of Health, one with Legislative Decree 116/92 and the other with the new Legislative Decree 26/2014, in accordance with the ARVO Statement for the Use of Animals in Ophthalmic and Vision Research. The procedures described below are part of a preclinical trial of a larger project aimed at developing new therapeutic approaches to restore vision in patients affected by pathologies that lead to photoreceptor degeneration.

Thirty commercial hybrid pigs [(Large White × Landrace) × Duroc] of both sexes, with weight between 16.6 and 38.2 kg (8–14 weeks old), were enrolled in this study. Thirteen ($n = 13$) pigs were treated, under general anesthesia, with 12 mg/kg IAA (CAS No. 64-69-7; Sigma Chemical Corp., St. Louis, MO, USA) as

previously described by Wang et al.,[28] to induce retinal degeneration. The remaining 17 untreated pigs ($n = 17$) were enrolled in the control group (CTR).

All animals were housed in multiple boxes with a 12:12-hour light:dark cycle and a minimum of 40 lux during the light period[26]; chains and wood were used as environmental enrichment.[30] The pigs were fed with standard commercial diet (PROGEO, Reggio Emilia, Italy) twice a day, with ad libitum water.

Sampling Procedure

Four weeks after IAA treatment, the VH$_{pIAA}$ were sampled during the surgical procedures, which were aimed to assess a novel therapeutic approach to restore vision. Before anesthesia, animals were fasted for 12 hours. After sedation with an intramuscular injection of tiletamine-zolazepam (Zoleti, l5 mg/kg; Virbac, Prague, Czech Republic), general anesthesia was induced with isoflurane (IsoFlo; Zoetis Italia s.r.l., Rome, Italy) administered through a mask in a 1:1 oxygen/air mixture, and maintained, after orotracheal intubation, with the same halogenated agent. From each animal, approximately 500 μL VH was collected upon vitrectomy into a sterile cryogenic tube and immediately frozen in liquid nitrogen, then stored at −80°C until analysis. The same procedures were performed on the CTR group animals.

Metabolomics by ^{1}H NMR

Humor samples were prepared for NMR analysis by means of centrifugation for 15 minutes at 18,630g and 4°C. Secondly, 350 μL supernatant with 350 μL bidistilled water was added to 100 μL of a D$_2$O solution of 3-(trimethylsilyl)-propionic-2,2,3,3-d4 acid sodium salt (TSP) 10 mM, used as NMR chemical-shift reference, buffered at pH 7.00 by means of 1 M phosphate buffer. Finally, each sample was centrifuged again under the above conditions and the supernatant underwent analysis.

^{1}H NMR spectra were recorded at 298 K with an AVANCE III spectrometer (Bruker, Milan, Italy) operating at a frequency of 600.13 MHz. Following Ventrella and colleagues,[12] the signals from broad resonances originating from large molecules were suppressed by a Carr-Purcell-Meiboom-Gill (CPMG) filter composed by 400 echoes with a τ of 400 μs and a 180° pulse of 24 μs, for a total filter of 330 ms. The deuterated water (HOD) residual signal was suppressed by means of presaturation. This was done by employing the cpmgpr1d sequence, part of the standard pulse sequence library. Each spectrum was acquired by summing up 256 transients using 32 K data points over a 7184-Hz spectral window, with an acquisition time of 2.28 seconds. In order to apply NMR as a quantitative technique, the recycle delay was set to 5 seconds, keeping in consideration the relaxation time of the protons under investigation. ^{1}H NMR spectra were baseline-adjusted by means of the peak detection according to the "rolling ball" principle[31] implemented in the baseline R package.[32] A linear correction was then applied to each spectrum, so as to make the points pertaining to the baseline randomly spread around zero. Differences in water and fiber content among samples were taken into consideration by probabilistic quotient normalization,[33] applied to the entire spectra array.

The signals were assigned by comparing simultaneously their chemical shift, multiplicity, fine structure, and signal relative intensity with the Human Metabolome Database[34] and Chenomx software library (ver 8.1; Chenomx, Inc., Edmonton, AB, Canada), both built on pure compounds under the experimental conditions of the present work, as detailed in Figures S1 through S13. For molecules giving rise to a singlet only, such as formate, fumarate, glycine, pyruvate, or
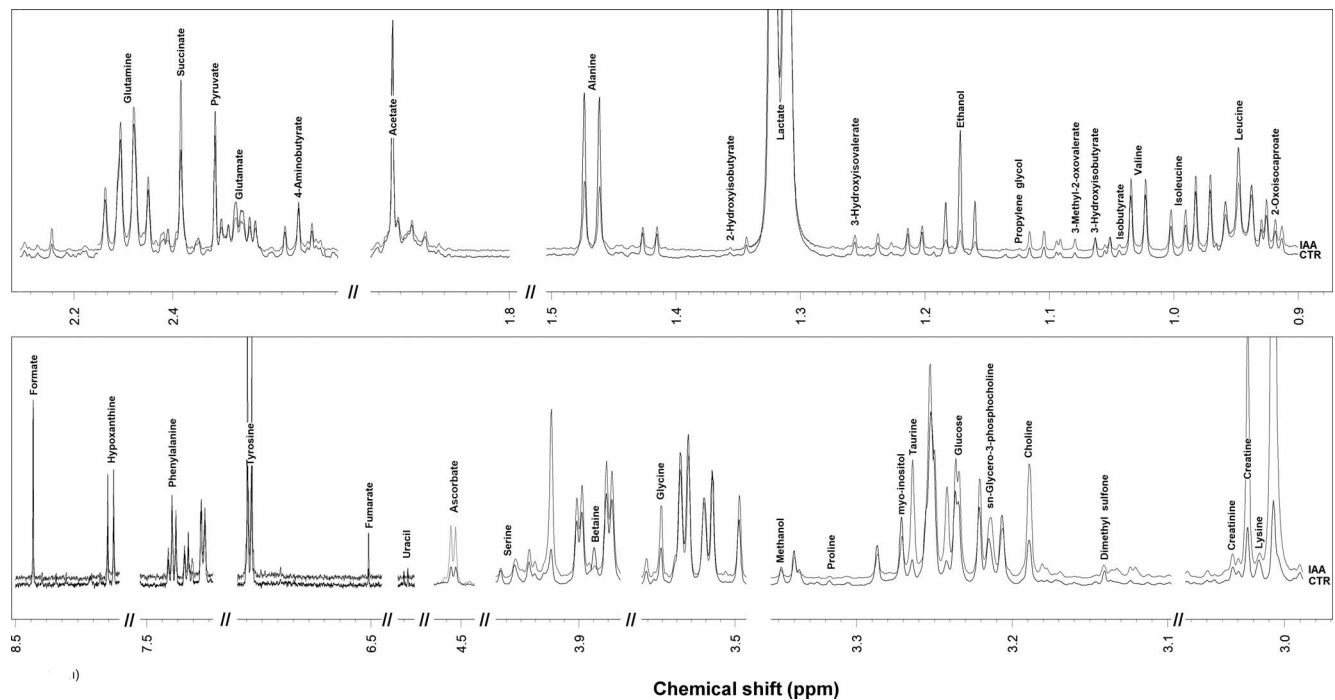
FIGURE 1. ^{1}H NMR spectra from one control and one treated sample, representative of all the registered spectra. The name of each molecule appears over the signal used for its quantification.

succinate, the assignment was accepted if the signal registered on the pure compound and the one under investigation were less than 0.6 Hz apart, as detailed in Figure S14. Integration of the signals was performed for each molecule by means of rectangular integration.[35]

Statistical Analysis

Data investigation was conducted on R platform.[36] In metabolomics evaluation, molecules whose concentration varied in relation to treatments were tested by a nonparametric Mann-Whitney test, by applying a continuity correction in the normal approximation for the P value. For this purpose, a significance limit P of 0.01 (confidence interval 99%) was accepted. To highlight the underlying trends characterizing the samples, the principal component analysis model in its robust version (rPCA) was built on the molecule concentrations, centered, and scaled to unity variance, according to Damisch.[37] This was done by taking advantage of the PCAHubert function of the R package rrcov.[38] For each rPCA model, we calculated the scoreplot, the projection of the samples in the principal component (PC) space, tailored to highlight the underlying structure of the data. Additionally, the correlation plot was calculated, relating the concentration of each variable to the components of the rPCA model, therefore tailored to highlight the most important molecules in determining the trends highlighted by the scoreplot.

RESULTS

VH samples collected during vitrectomy proved to be suitable for the chosen analytic technique, as already reported in the literature.[15]

^{1}H NMR spectra of VH of the CTR and IAA groups are reported in Figure 1. Forty molecules were identified and quantified in all of the analyzed samples, and the results including P values and trends are summarized the Table.

From a quantitative point of view, both in the CTR and IAA groups, lactate was the most concentrated metabolite, followed by glucose, glutamine, and ascorbate (Table). Other metabolites identified were the amino acids, with glutamine being the most representative. The comparison between the two experimental groups highlighted 17 significantly different molecules ($P < 0.01$). In order to obtain an overview of underlying trends, the above-mentioned 17 molecules were employed as basis for an rPCA model, shown in Figure 2. Along PC 1 of its scoreplot (Fig. 2A), representing as much as 87.2% of the entire sample variability explained by the PCA, the two groups appeared as significantly separated ($P < 0.01$).

The molecules that mainly drove such separation, with a correlation between importance over PC 1 and concentration higher than 0.8 (Fig. 2B), were glycine, taurine, choline, creatine, sn-glycero-3-phosphocholine, 4-aminobutyrate, hypoxanthine, and fumarate, more concentrated in CTR group.

DISCUSSION

In recent years, the use of pigs for non- or preclinical ophthalmologic trials has been exponentially increasing as proven by the literature.[39] One of the biggest issues of enrolling animal models of any kind in such studies is the lack of extensive characterization that often affects the translational potential.[40] This is why extensive characterization is key to interpret data and thus to obtain robust results, and to comply with the 3R principles for animal experimentation.[41] Moreover, the possibility to highlight biomarkers of pathology in biological fluids of animal models may assist correlation with the actual human pathology, validating the model itself.

To the best of the authors' knowledge, this is the first metabolomics characterization of the porcine VH by means of ^{1}H NMR spectroscopy, a platform characterized by lower sensitivity compared to others usually employed for metabolomics investigations, counterbalanced by a high reproducibility and inherent simplicity.[42] Such a physiological profile

TABLE. Concentration of the Molecules Quantified by ^{1}H NMR in VH (m/M). The Concentrations Are Expressed as Median (Interquartile Range)

Molecules	CTR ($n = 17$)	IAA ($n = 13$)	P Value	Trend
Lactate	15.8 (10.6)	8.72 (1.87)	0.0001*	↓
Glucose	1.40 (4.58×10^{-1})	2.68 (7.04×10^{-1})	0.0005*	↑
Glutamine	1.35 (2.21×10^{-1})	1.72 (3.17×10^{-1})	0.0003*	↑
Ascorbate	1.16 (1.09×10^{-1})	1.52 (2.88×10^{-1})	0.6206	
Taurine	5.07×10^{-1} (6.52×10^{-1})	1.67×10^{-1} (4.19×10^{-2})	0.0061*	↓
myo-Inositol	4.28×10^{-1} (3.75×10^{-1})	3.79×10^{-1} (1.68×10^{-1})	0.8506	
Serine	4.05×10^{-1} (1.46×10^{-1})	3.45×10^{-1} (4.75×10^{-2})	0.0364	
Creatine	3.55×10^{-1} (3.77×10^{-1})	1.76×10^{-1} (4.90×10^{-2})	0.0039*	↓
Glutamate	3.22×10^{-1} (4.69×10^{-1})	1.09×10^{-1} (4.77×10^{-2})	0.0144	
Acetate	2.84×10^{-1} (1.64×10^{-1})	1.77 (4.19)	0.0687	
Alanine	2.72×10^{-1} (1.40×10^{-1})	2.05×10^{-1} (7.30×10^{-2})	0.0034*	↓
Valine	2.14×10^{-1} (5.39×10^{-2})	1.44×10^{-1} (2.92×10^{-2})	0.0015*	↓
Lysine	2.00×10^{-1} (8.37×10^{-2})	1.09×10^{-1} (4.47×10^{-2})	0.0014*	↓
Leucine	1.82×10^{-1} (5.64×10^{-2})	1.36×10^{-1} (5.71×10^{-2})	0.0095*	↓
Formate	1.81×10^{-1} (5.21×10^{-2})	1.84×10^{-1} (7.42×10^{-2})	0.2412	
Tyrosine	1.78×10^{-1} (7.22×10^{-2})	1.24×10^{-1} (6.64×10^{-2})	0.0364	
Glycine	1.60×10^{-1} (9.48×10^{-2})	4.47×10^{-2} (1.74×10^{-2})	0.0021*	↓
Pyruvate	1.44×10^{-1} (8.22×10^{-2})	1.96×10^{-1} (1.51×10^{-1})	0.1026	
Phenylalanine	1.36×10^{-1} (3.90×10^{-2})	1.06×10^{-1} (3.10×10^{-2})	0.028	
Succinate	1.35×10^{-1} (6.13×10^{-2})	8.94×10^{-2} (4.56×10^{-2})	0.0011*	↓
Isoleucine	1.15×10^{-1} (4.49×10^{-2})	6.53×10^{-2} (4.81×10^{-2})	0.0054*	↓
Hypoxanthine	8.35×10^{-2} (7.58×10^{-2})	2.67×10^{-2} (1.02×10^{-2})	0.0018*	↓
4-Aminobutyrate	8.15×10^{-2} (1.43×10^{-1})	1.92×10^{-2} (1.22×10^{-2})	0.0003*	↓
Ethanol	7.80×10^{-2} (7.36×10^{-2})	6.53×10^{-2} (7.20×10^{-2})	0.4639	
Creatinine	7.50×10^{-2} (1.40×10^{-2})	1.08×10^{-1} (5.43×10^{-2})	0.0901	
Betaine	6.74×10^{-2} (2.26×10^{-2})	6.52×10^{-2} (1.21×10^{-2})	0.4388	
2-Oxoisocaproate	6.46×10^{-2} (1.39×10^{-2})	8.06×10^{-2} (2.37×10^{-2})	0.0144	
Choline	5.89×10^{-2} (5.90×10^{-2})	3.23×10^{-2} (8.68×10^{-3})	0.0005*	↓
3-Hydroxyisobutyrate	3.91×10^{-2} (6.70×10^{-3})	3.41×10^{-2} (1.93×10^{-2})	0.9499	
3-Methyl-2-oxovalerate	3.77×10^{-2} (1.65×10^{-2})	4.99×10^{-2} (1.19×10^{-2})	0.0295	
Methanol	3.37×10^{-2} (2.03×10^{-2})	4.04×10^{-2} (1.11×10^{-2})	0.6603	
sn-Glycero-3-phosphocholine	3.12×10^{-2} (3.51×10^{-2})	1.55×10^{-2} (2.79×10^{-3})	0.0069*	↓
Uracil	2.54×10^{-2} (1.45×10^{-2})	1.99×10^{-2} (1.41×10^{-2})	0.1609	
Dimethyl sulfone	1.90×10^{-2} (1.19×10^{-2})	5.92×10^{-2} (7.31×10^{-2})	0.0824	
Proline	1.52×10^{-2} (1.75×10^{-2})	1.21×10^{-3} (2.68×10^{-2})	0.0788	
3-Hydroxyisovalerate	1.35×10^{-2} (3.99×10^{-3})	1.41×10^{-2} (6.91×10^{-3})	0.2329	
Fumarate	1.13×10^{-2} (1.16×10^{-2})	6.61×10^{-3} (2.63×10^{-3})	0.0024*	↓
Isobutyrate	9.79×10^{-3} (5.92×10^{-3})	1.02×10^{-2} (6.21×10^{-3})	0.7064	
2-Hydroxyisobutyrate	5.01×10^{-3} (2.71×10^{-3})	8.74×10^{-3} (8.44×10^{-3})	0.5165	
Propylene glycol	3.52×10^{-3} (6.03×10^{-3})	2.42×10^{-3} (2.45×10^{-3})	0.2859	

* Molecules showing statistical differences between CTR and IAA ($P < 0.01$).

was used as reference for comparison with the VH metabolome of the swine model of photoreceptor degeneration induced by IAA. This model is indeed still lacking in-depth characterization, and the description of its VH metabolome may provide important information for future ophthalmologic experimental trials.

It is worth remarking on the importance of acknowledging the precise VH collection site since the different vitreous areas specifically reflect different metabolic activities influenced by the surrounding structures.[15] The samples analyzed in the present study were collected upon vitrectomy and represent the portion of VH directly in contact with the retina, called the cortical area, providing direct insight into the retinal metabolic activity. The reproducibility of the sampling/handling technique was confirmed by the coherent identification and quantification, in all the samples, of the same 40 molecules as reported in the Table.

The physiological composition of the swine VH_p shows resemblance with what has already been reported in the literature for humans[11] and animals,[15] with lactate being the most abundant metabolite. This is supposedly related to the limited availability of oxygen within the eye and high consumption rates in the retina that lead to anaerobic glycolysis with subsequent production of lactate.[15] The other most abundant metabolites were glucose, glutamine, and ascorbate, as already reported, for example, in the goat.[15] Glutamine seems to characterize the same vitreous area, the cortical area, also in the goat.[15] This molecule represents the main metabolite of glutamate, which is the most important excitatory neurotransmitter in the retina and needs to be converted by glutamine synthetase in order to avoid neurotoxicity.[15,43] Ascorbate seems to accumulate in the ocular tissues in order to prevent oxidative damage,[44] and its concentration is from 1 to 10 times higher than in the blood/plasma.[45,46] It also seems to be involved in sunlight protection, as it is more abundant in diurnal rather than nocturnal animals.[46]

The comparison between CTR and IAA groups has highlighted 17 molecules showing statistical differences, out of which only glucose and glutamine increased upon induction of photoreceptor degeneration. It is important to stress that systemic administration of IAA leads to the inhibition of
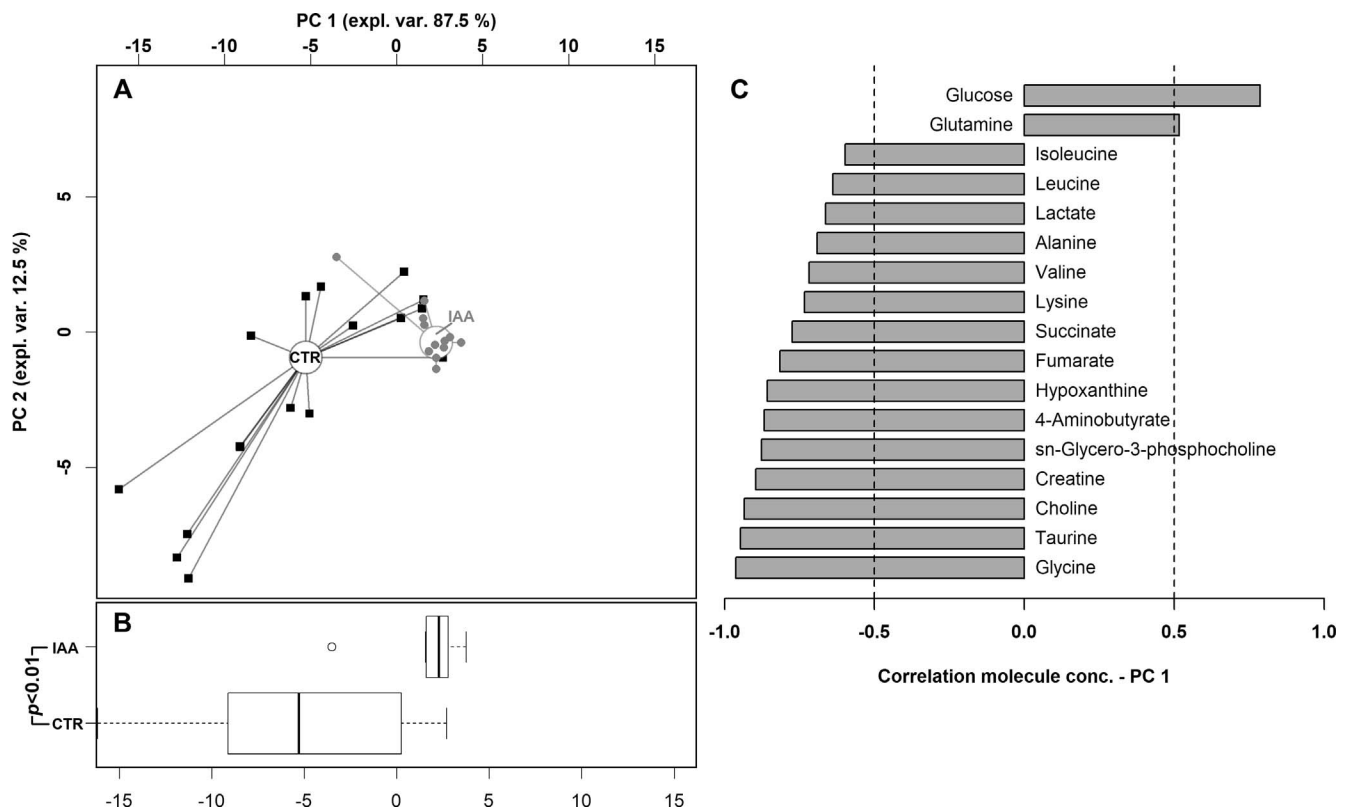
FIGURE 2. rPCA model built on the space constituted by the concentration of the molecules showing a statistically significant difference between the CTR and IAA groups. In the scoreplot (**A**), samples from the two groups are represented with *squares* and *circles*, respectively. The *wide, empty circles* represent the median of the samples. The position of the subjects along PC 1 is summarized in the boxplot (**B**). The loading plot (**C**) reports the correlation between the concentration of each substance and its importance over PC 1. Significant correlations ($P < 0.01$) are highlighted with *gray bars*.

anaerobic glycolysis,[27] with subsequent degeneration of the photoreceptor as one of the most sensitive cells.[21] Therefore, the explanation for the increase in glucose concentrations upon IAA administration seems to be clear, as a direct result of the relative inability to break it down for energy production. The other metabolite that showed a significant increasing trend was glutamine, the product of glutamate metabolism, which, in the retina, takes place in the Müller cells thanks to the action of the glutamine synthetase enzyme.[47] When exposed to hypoxic damage, the retina shows an increase in glutamine concentrations due to the impossibility of the photoreceptors to correctly uptake glutamine from the extracellular matrix.[48] Most importantly, Scott and colleagues[21] demonstrated how systemic administration of IAA leads to proliferation of the Müller cells; therefore it is likely that higher levels of glutamine reflect higher metabolic activity of these cells and their enzymes.

The 15 molecules that significantly decreased in the IAA group included lactate, 4-amynobutyrate, hypoxanthine, dicarboxylic acids (succinate and fumarate), amino acids and their derivatives (creatine, alanine, valine, lysine, leucine, glycine, taurine, and isoleucine), and choline and its precursor sn-glycero-3-phosphocholine. As for what was already discussed regarding glucose, the decrease in lactate levels seems the obvious consequence of the inhibition of anaerobic glycolysis induced by the administered chemical compound. Indeed, as already stated, lactate is the main product of this metabolic pathway.[49] 4-Amynobutyrate, also known as GABA, is a neurotransmitter produced in retinal horizontal cells using glutamate as substrate.[50] Lower concentrations of GABA in the IAA group may be related to the low bioavailability of some precursor amino acids of the neurotransmitters, such as leucine, isoleucine, and taurine, that are indeed lower in this group. The same hypothesis can be proposed for the highlighted lower levels of another neurotransmitter precursor such as choline. When discussing the findings regarding GABA, it is also important to acknowledge the high levels of glutamine, which is a precursor in GABA production.[47] It is indeed possible to hypothesize a potential inhibition to intracellular transport of glutamine leading to higher levels of precursor and lower levels of neurotransmitter. Further validation seems to be found in the levels of succinate, significantly lower in the IAA group, since it is a metabolite of GABA.[50] Alongside fumarate, succinate also represents a reaction intermediate in the Krebs cycle, that provides the outer retina with enough ATP for its metabolic requirements and phototransduction.[51] A decrease in these molecules may therefore strengthen the idea of an overall damage to the retinal structures and their metabolic pathways. Discussion regarding the overall decrease in amino acid levels can be complicated as they are involved in a variety of proteome-related processes.[12] Nonetheless, this finding is a further reflection of the photoreceptor damage induced by IAA, as one of the roles of this molecule includes photoreceptor protection and development.[52] Moreover, it has already been described how physiological VH is usually rich in amino acids as shed byproducts of retinal cell turnover.[53] It is therefore likely that the induced decrease in photoreceptor metabolic activity may have led to reduced levels of free amino acids. The same hypothesis can be made for the reduction in hypoxanthine levels, related to an overall reduced retinal metabolism, as reported in a rat model of ischemic retinopathy.[54]

In conclusion, this work represents the first characterization of the VH metabolome in young physiological standard pigs and in the IAA-induced model of photoreceptor degeneration through ^{1}H NMR spectroscopy. The physiological characterization itself will provide a standard reference for future ophthalmologic non- and preclinical trials, potentially helping data interpretation and analysis. On the other hand, the findings regarding the IAA group represent a pivotal refinement of this important model and may contribute to more aware and responsible enrollment of such porcine models in future studies. Indeed, as for every animal model, in-depth overall characterization is necessary in order to achieve high translational value and robust and repeatable data.

Acknowledgments

References

1. Bishop PN, Holmes DF, Kadler KE, McLeod D, Bos KJ. Age-related changes on the surface of vitreous collagen fibrils. *Invest Ophthalmol Vis Sci*. 2004;45:1041–1046.

2. Bos KJ, Holmes DF, Meadows RS, Kadler KE, McLeod D, Bishop PN. Collagen fibril organisation in mammalian vitreous by freeze etch/rotary shadowing electron microscopy. *Micron*. 2001;32:301–306.

3. Bishop PN. Structural macromolecules and supramolecular organisation of the vitreous gel. *Prog Retin Eye Res*. 2000;19:323–344.

4. Lazarus HS, Hageman GS. In situ characterization of the human hyalocyte. *Arch Ophthalmol*. 1994;112:1356–1362.

5. Rosa MF, Scano P, Noto A, et al. Monitoring the modifications of the vitreous humor metabolite profile after death: an animal model. *BioMed Res Int*. 2015;2015:627201.

6. Hosoya K, Tomi M. Advances in the cell biology of transport via the inner blood-retinal barrier: establishment of cell lines and transport functions. *Biol Pharm Bull*. 2005;28:1–8.

7. Mains J, Tan LE, Zhang T, Young L, Shi R, Wilson C. Species variation in small molecule components of animal vitreous. *Invest Ophthalmol Vis Sci*. 2012;53:4778–4786.

8. Cunha-Vaz JG. The blood-retinal barriers system. Basic concepts and clinical evaluation. *Exp Eye Res*. 2004;78:715–721.

9. Barba I, Garcia-Ramírez M, Hernández C, et al. Metabolic fingerprints of proliferative diabetic retinopathy: an 1H-NMR-based metabonomic approach using vitreous humor. *Invest Ophthalmol Vis Sci*. 2010;51:4416–4421.

10. Petrash JM. Aging and age-related diseases of the ocular lens and vitreous body. *Invest Ophthalmol Vis Sci*. 2013;54:ORSF54–ORSF59.

11. Young SP, Nessim M, Falciani F, et al. Metabolomic analysis of human vitreous humor differentiates ocular inflammatory disease. *Mol Vis*. 2009;15:1210–1217.

12. Ventrella D, Laghi L, Barone F, Elmi A, Romagnoli N, Bacci ML. Age-related 1H NMR characterization of cerebrospinal fluid in newborn and young healthy piglets. *PLoS One*. 2016;11:e0157623.

13. Musteata M, Nicolescu A, Solcan G, Deleanu C. The 1H NMR profile of healthy dog cerebrospinal fluid. *PLoS One*. 2013;8:e81192.

14. Merrifield CA, Lewis M, Claus SP, et al. A metabolic system-wide characterisation of the pig: a model for human physiology. *Mol Biosyst*. 2011;7:2577–2588.

15. Locci E, Scano P, Rosa MF, et al. A metabolomic approach to animal vitreous humor topographical composition: a pilot study. *PLoS One*. 2014;9:e97773.

16. Ortmann J, Markwerth P, Madea B. Precision of estimating the time since death by vitreous potassium-comparison of 5 different equations. *Forensic Sci Int*. 2016;269:1–7.

17. Panova IG, Sharova NP, Dmitrieva SB, Levin PP, Tatikolov AS. Characterization of the composition of the aqueous humor and the vitreous body of the eye of the frog Rana temporaria L. *Comp Biochem Physiol A Mol Integr Physiol*. 2008;151:676–681.

18. Koeberle MJ, Hughes PM, Skellern GG, Wilson CG. Pharmacokinetics and disposition of memantine in the arterially perfused bovine eye. *Pharm Res*. 2006;23:2781–2798.

19. Mains J, Wilson CG, Urquhart A. ToF-SIMS analysis of dexamethasone distribution in the isolated perfused eye. *Invest Ophthalmol Vis Sci*. 2011;52:8413–8419.

20. Yan H, Ahmed AS, Han J, Cui J, Yu J. A vitreous hemorrhage animal model in rabbits using force percussion injury. *Curr Eye Res*. 2009;34:717–726.

21. Scott PA, Kaplan HJ, Sandell JH. Anatomical evidence of photoreceptor degeneration induced by iodoacetic acid in the porcine eye. *Exp Eye Res*. 2011;93:513–527.

22. Reisenhofer MH, Balmer JM, Enzmann V. What can pharmacological models of retinal degeneration tell us? *Curr Mol Med*. 2017;17:100–107.

23. Petters RM, Alexander CA, Wells KD, et al. Genetically engineered large animal model for studying cone photoreceptor survival and degeneration in retinitis pigmentosa. *Nat Biotechnol*. 1997;15:965–970.

24. Scott PA, de Castro JPF, DeMarco PJ, et al. Progression of Pro23His retinopathy in a miniature swine model of retinitis pigmentosa. *Trans Vis Sci Tech*. 2017;6(2):4.

25. Noel JM, Fernandez de Castro JP, Demarco PJ, et al. Iodoacetic acid, but not sodium iodate, creates an inducible swine model of photoreceptor damage. *Exp Eye Res*. 2012;97:137–147.

26. Barone F, Nannoni E, Elmi A, et al. Behavioral assessment of vision in pigs. *J Am Assoc Lab Anim Sci*. 2018;57:350–356.

27. Winkler BS, Sauer MW, Starnes CA. Modulation of the Pasteur effect in retinal cells: implications for understanding compensatory metabolic mechanisms. *Exp Eye Res*. 2003;76:715–723.

28. Wang W, de Castro JF, Vukmanic E, et al. Selective rod degeneration and partial cone inactivation characterize an iodoacetic acid model of swine retinal degeneration. *Invest Ophthalmol Vis Sci*. 2011;52:7917–7923.

29. Hafezi F, Grimm C, Simmen BC, Wenzel A, Remé CE. Molecular ophthalmology: an update on animal models for retinal degenerations and dystrophies. *Br J Ophthalmol*. 2000;84:922–927.

30. Nannoni E, Sardi L, Vitali M, et al. Effects of different enrichment devices on some welfare indicators of post-weaned undocked piglets. *Appl Anim Behav Sci*. 2016;184:25–34.

31. Kneen MA, Annegarn HJ. Algorithm for fitting XRF, SEM and PIXE X-ray spectra backgrounds. *Nucl Instrum Methods Phys Res B*. 1996;109–110:209–213.

32. Liland KH, Almøy T, Mevik BH. Optimal choice of baseline correction for multivariate calibration of spectra. *Appl Spectrosc*. 2010;64:1007–1016.

33. Dieterle F, Ross A, Schlotterbeck G, Senn H. Probabilistic quotient normalization as robust method to account for dilution of complex biological mixtures. Application in 1H NMR metabonomics. *Anal Chem*. 2006;78:4281–4290.

34. Wishart DS, Tzur D, Knox C, et al. HMDB: The Human Metabolome Database. *Nucleic Acids Res*. 2007;35:D521–D526.

35. Ostebee A, Zorn P. *Calculus from Graphical, Numerical, and Symbolic Points of View*. 2nd ed. Houghton Mifflin School; 2002.

36. Ihaka R, Gentleman R. R: a language for data analysis and graphics. *J Comput Graph Stat*. 1996;5:299–314.

37. Damisch H, Bann S. Hubert Damisch and Stephen Bann: a conversation. *Oxf Art J*. 2005;28:155–181.

38. Todorov V, Filzmoser P. An object-oriented framework for robust multivariate analysis. *J Stat Softw*. 2009;32:1–47.

39. Pennesi ME, Neuringer M, Courtney RJ. Animal models of age related macular degeneration. *Mol Aspects Med*. 2012;33:487–509.

40. Schulz JB, Cookson MR, Hausmann L. The impact of fraudulent and irreproducible data to the translational research crisis - solutions and implementation. *J Neurochem*. 2016;139(suppl 2):253–270.

41. Tannenbaum J, Bennett BT. Russell and Burch's 3Rs then and now: the need for clarity in definition and purpose. *J Am Assoc Lab Anim Sci*. 2015;54:120–132.

42. Laghi L, Picone G, Capozzi F. Nuclear magnetic resonance for foodomics beyond food analysis. *Trends Analyt Chem*. 2014;59:93–102.

43. Zeng K, Xu H, Chen K, et al. Effects of taurine on glutamate uptake and degradation in Müller cells under diabetic conditions via antioxidant mechanism. *Mol Cell Neurosci*. 2010;45:192–199.

44. Wei W, Li L, Zhang Y, et al. Vitamin C protected human retinal pigmented epithelium from oxidant injury depending on regulating SIRT1. *ScientificWorldJournal*. 2014;2014:750634.

45. Linster CL, Van Schaftingen E. Vitamin C. Biosynthesis, recycling and degradation in mammals. *FEBS J*. 2007;274:1–22.

46. Rose RC, Bode AM. Ocular ascorbate transport and metabolism. *Comp Biochem Physiol A*. 1991;100:273–285.

47. Bringmann A, Pannicke T, Biedermann B, et al. Role of retinal glial cells in neurotransmitter uptake and metabolism. *Neurochem Int*. 2009;54:143–160.

48. Napper GA, Pianta MJ, Kalloniatis M. Localization of amino acid neurotransmitters following in vitro ischemia and anoxia in the rat retina. *Vis Neurosci*. 2001;18:413–427.

49. Winkler BS. Glycolytic and oxidative metabolism in relation to retinal function. *J Gen Physiol*. 1981;77:667–692.

50. Kalloniatis M, Tomisich G. Amino acid neurochemistry of the vertebrate retina. *Prog Retin Eye Res*. 1999;18:811–866.

51. Panfoli I, Calzia D, Ravera S, et al. Extramitochondrial tricarboxylic acid cycle in retinal rod outer segments. *Biochimie*. 2011;93:1565–1575.

52. Jiang Z, Bulley S, Guzzone J, Ripps H, Shen W. The modulatory role of taurine in retinal ganglion cells. *Adv Exp Med Biol*. 2013;775:53–68.

53. Skeie JM, Mahajan VB. Proteomic interactions in the mouse vitreous-retina complex. *PLoS One*. 2013;8:e82140.

54. Paris LP, Johnson CH, Aguilar E, et al. Global metabolomics reveals metabolic dysregulation in ischemic retinopathy. *Metabolomics*. 2016;12:15.

Investigative Ophthalmology & Visual Science